

# Chapter 13

## Drug Ratio-Dependent Antagonism: A New Category of Multidrug Resistance and Strategies for Its Circumvention

Troy O. Harasym, Barry D. Liboiron, and Lawrence D. Mayer

### Abstract

A newly identified form of multidrug resistance (MDR) in tumor cells is presented, pertaining to the commonly encountered resistance of cancer cells to anticancer drug combinations at discrete drug:drug ratios. In vitro studies have revealed that whether anticancer drug combinations interact synergistically or antagonistically can depend on the ratio of the combined agents. Failure to control drug ratios in vivo due to uncoordinated pharmacokinetics could therefore lead to drug resistance if tumor cells are exposed to antagonistic drug ratios. Consequently, the most efficacious drug combination may not occur at the typically employed maximum tolerated doses of the combined drugs if this leads to antagonistic ratios in vivo after administration and resistance to therapeutic effects of the drug combination. Our approach to systematically screen a wide range of drug ratios and concentrations and encapsulate the drug combination in a liposomal delivery vehicle at identified synergistic ratios represents a means to mitigate this drug ratio-dependent MDR mechanism. The in vivo efficacy of the improved agents (CombiPlex formulations) is demonstrated and contrasted with the decreased efficacy when drug combinations are exposed to tumor cells in vivo at antagonistic ratios.

**Key words:** Multidrug resistance, Synergy, Antagonism, Ratiometric, Drug delivery, Liposomes, Drug screening, Median effect analysis

---

### 1. Introduction

Combination chemotherapy has been the cornerstone of cancer therapy for over 40 years. Improvements in outcomes for childhood leukemia highlight how development of combination treatments has led to dramatic increases in efficacy over single agents. From response rates of 40% and no cures with methotrexate alone, greater than 95% complete response and 75–80% cure rates could be achieved when methotrexate was administered in combination with

asparaginase, daunorubicin, and cytarabine (1, 2). Yet in contrast to these advancements in leukemia, achieving a cure for the majority of solid tumors remains elusive (3). Response rates of pancreatic, esophageal, and recurrent ovarian cancer are still below 20% despite the massive efforts and resources that have been expended to develop superior combination therapies for these indications (4). The failure of many combinations to achieve complete remissions in the majority of cases is frequently attributed to multidrug resistance (MDR), a phenomenon that allows tumor cells to survive and/or flourish under considerable challenge from exogenous cytotoxic agents. Much attention has been paid to identified resistance factors such as P-glycoprotein (Pgp) and multidrug resistance-associated protein (MRP), altered apoptosis mechanisms as well as modifications in enzyme activity (e.g., topoisomerase II, glutathione-S-transferase) in an attempt to elucidate and mitigate these mechanisms in order to improve efficacy (5–8). Efforts to specifically target and neutralize these mechanisms, however, have been largely ineffective (9, 10). Thus, development of new treatments, identification of synergistic drug interactions, and refinement of treatment protocols remain the main strategies for mitigating the effects of MDR and improving the treatment outcomes of cancer patients.

---

## **2. Drug–Drug Antagonism: A New Form of MDR**

The discovery of favorable drug–drug interactions in combination chemotherapy remains an active field of basic and clinical research. Some researchers have successfully combined agents with different mechanisms of action in which multiple sites in biochemical pathways are attacked, resulting in synergy (11), while others have demonstrated synergy by combining agents that target the same pathway(s) (12–14). Identification and characterization of synergistic drug interactions therefore remains a very active area of research and has resulted in the introduction of several new combination chemotherapies in the past decade (15–18). Intrinsic in the discovery of drug:drug synergy, yet often ignored in these studies, is the identification of drug:drug antagonism, in which the efficacy of the two agents is impaired such that the cytotoxicity of the combined agents is less than what would be expected for the additive activities of the individual agents (19, 20).

Extolling the discovery of drug–drug synergy while ignoring the existence of drug–drug antagonism under certain conditions for a given combination can, in fact, lead to compromised efficacy. Exposure of tumor cells to two drugs in combination at a certain ratio and concentration can lead to one of three outcomes: synergistic,

additive, or antagonistic activity. Thus, while the literature is quick to identify drug combinations that have augmented activity *in vitro*, little attention is paid to whether the conditions used *in vitro* (e.g., drug ratio and concentration) are pharmacologically relevant *in vivo*. Consequently, when synergy is observed, this represents ratios at which tumor cells are *susceptible* to the combination, but historically identification and avoidance of antagonistic ratios at which tumor cells are *resistant* to the combined agents is largely ignored. From an empirical perspective, drug:drug antagonism is a form of MDR in that the cellular response is inexplicably less than what would be minimally expected (i.e., additivity); it affects multiple structurally disparate chemotherapeutic agents and it is known to occur across a wide variety of tumor types. For reasons likely related to the interconnected nature of pathway biochemistry and cellular biology, a particular cell line may be less susceptible to a specific drug combination presented at a certain ratio, yet this resistance mechanism can frequently be bypassed through exposure of the same drugs at a different ratio.

Further complicating this phenomenon is that some studies reveal that activity of a particular drug ratio may also be concentration-dependent; exhibiting synergy at one total drug concentration and producing additive or antagonistic results at other concentrations. Since drug concentrations decrease over time after *in vivo* administration, it is important to identify and utilize ratios of drugs that behave synergistically over a broad range of drug concentrations, while avoiding those combinations that exhibit either broad ratio or concentration-specific antagonism. While these ratios can be readily identified through a variety of drug screening techniques, the translation of such information from *in vitro* cytotoxicity studies to *in vivo* efficacy studies is difficult to achieve using the current treatment paradigm for antitumor combination chemotherapy.

### **2.1. Current Combination Therapy Development**

The empiric process used to advance new combinations in the clinic has evolved little since the concept of combination chemotherapy was pioneered by Frei and coworkers in the 1960s (21). In this process, individual drugs in a combination are escalated to the maximum dose where aggregate toxicity is tolerable with the expectation that maximum therapeutic activity will be achieved at the maximum dose of each agent.

Conventional combination therapy, however, frequently fails to account for disparate physiochemical properties of each drug component that will typically result in the rapid and independent distribution and elimination of each agent. Without a means to control the pharmacokinetics (PKs) of each drug, their unique clearance properties will lead to rapidly changing and uncontrolled drug:drug ratios after administration. Therefore, over a

short period of time, combinations administered as an unbridled cocktail can be present at synergistic, additive, and/or antagonistic ratios if the combination exhibits drug ratio-dependent interactions. Consequently, failure to account for and control drug ratios in the application of drug combinations *in vivo* could lead to the exposure of tumor cells to antagonistic drug ratios, leading to empirical MDR and corresponding loss of therapeutic activity. Encouragingly, the role of synergistic and antagonistic drug interactions in the mitigation and emergence of MDR is gaining interest in the current literature for a variety of disease states (22–26).

*2.1.1. Case Study:  
Gemcitabine and Cisplatin  
Pharmacokinetics*

The combination of gemcitabine and cisplatin is instructive in highlighting the changes in plasma concentrations and drug ratios that occur following coadministration of the two drugs, using pharmacokinetic parameters presented in Table 13.1. Gemcitabine is infused first over a period of 30 min at a total dose of 1,250 mg/m<sup>2</sup>, followed by a 1-h infusion of saline to minimize renal toxicity from cisplatin. Cisplatin is then administered at 100 mg/m<sup>2</sup> in 1 L of saline over a 1-h infusion time. The average terminal half-lives of gemcitabine and cisplatin are 69 and 33 min, respectively (product monographs; Eli Lilly 1999, Mayne Pharma, 2003), which represents a 2.1-fold difference in plasma elimination rates.

Using the aforementioned PK parameters, volumes of distribution (Table 13.1) and accounting for the differences in both administration start times and durations between gemcitabine and cisplatin, the drug concentrations and associated drug:drug ratios can be estimated. Upon completion of the cisplatin infusion,

**Table 13.1**  
**A typical treatment regimen using the combination of cisplatin and gemcitabine for advanced non-small cell lung cancer (NSCLC)**

Drug	Drug dose <sup>a</sup> (mg/m <sup>2</sup> /day)	Administration	Volume of distribution (L/m <sup>2</sup> )	Terminal half-life (~min) <sup>b</sup>
Gemcitabine	1,250 on days 1 and 8	IV in 250 mL of NS over 30 min.	50	42–96
Cisplatin	100 on day 1	Prehydrate with 1,000 mL NS over 60 min then cisplatin IV in 1,000 mL NS over 60 min.	41	20–45

Note: Gemcitabine is administered first

<sup>a</sup>Drug dose and treatment schedule from BC Cancer Agency chemotherapy protocol (LUAVPG) available online at <http://www.bccancer.bc.ca/HPI/ChemotherapyProtocols/Lung/default.htm>

<sup>b</sup>From BC Cancer Agency drug manual and Gemzar and Platinol-AQ product monographs

the respective gemcitabine and cisplatin plasma concentrations are 20 and 2  $\mu\text{M}$ , reflecting a 10:1 molar ratio. At 30 min after completion of the cisplatin infusion, only 50% of the postdistribution cisplatin concentration ( $\sim 1 \mu\text{M}$ ) and 72% of the postdistribution gemcitabine concentration ( $\sim 14 \mu\text{M}$ ) is expected to remain in the plasma. Hence, the rapidly decreasing plasma drug concentrations will quickly lead to levels that fall below effective cellular cytotoxic values for cisplatin (e.g., the concentration of drug required to kill 50% of target cells in vitro, IC<sub>50</sub> value, for gemcitabine and cisplatin in a A549 human non-small cell lung cancer cell line is 0.007 and 4.2  $\mu\text{M}$ , respectively), highlighting that increased drug elimination results in decreased cell kill fractions. Furthermore, given that approximately 50% of the cisplatin and 28% of the gemcitabine is eliminated from the plasma every 30 min postadministration, the gemcitabine:cisplatin ratio increases by 1.44-fold over that time period. Specifically, at  $t=0$  the molar ratio of gemcitabine:cisplatin is approximately 10:1, whereas after 30 and 60 min, the gemcitabine:cisplatin molar ratio would increase to approximately 14:1 and 21:1, respectively, reflecting a doubling of the original gemcitabine:cisplatin ratio. By 4 h, the gemcitabine:cisplatin ratio will be approximately 185:1, an increase nearly 20-fold from the starting drug ratio. In view of the evidence of drug ratio-dependent synergy in vitro and in vivo for several drug combinations (13, 14, 27–29), careful consideration should be given to ensure that the in vitro methodologies utilized to evaluate drug combinations for synergy take these pharmacological properties into account. Failure to do so could result in concluding that a given drug combination is synergistic when, in fact, drug ratios and concentrations reflecting those exposed to tumor cells in vivo could be highly antagonistic and susceptible to drug ratio-dependent MDR.

---

### **3. In Vivo Avoidance of Drug Ratio-Dependent MDR: The CombiPlex Approach**

We have developed an approach in which we identify antagonistic drug:drug ratios for a particular drug combination in vitro and subsequently package the two drugs in a drug delivery vehicle such that a concentration-independent synergistic ratio of the two drugs is delivered directly to the tumor site and antagonistic ratios are avoided. Subsequent in vivo efficacy studies are used to confirm the translation of in vitro drug synergy relationships to actual efficacy improvements over the individual agents, the free drug cocktail and, most importantly, significant increases in efficacy over the two drugs delivered in a vehicle at an antagonistic ratio.

This review will detail the most common algorithms used to assess ratio-dependent drug:drug synergy/antagonism as well as methods to fix desirable drug ratios in vivo and evaluate the efficacy of fixed ratio combination agents in a variety of tumor xenografts. This ratiometric dosing approach to combination chemotherapy represents a means to augment the in vivo efficacy of combination therapies by maximizing tumor exposure to drugs at their synergistic ratios and avoidance of antagonistic ratios at which the ratio-dependent MDR mechanisms are active.

**3.1. Drug Synergy/  
Antagonism  
Screening:  
Experimental Design  
Considerations**

The most efficient and accurate means to evaluate drug interactions is through in vitro cytotoxicity assays, and several approaches can be taken when structuring how agents are combined experimentally in order to evaluate drug combinations for synergy in vitro. In general, these approaches evaluate drug combinations based upon (1) a nonconstant ratio design where the drug concentrations are chosen arbitrarily based on the features such as the relative in vitro antitumor potencies of the individual agents or plasma concentrations achieved clinically (30, 31), or (2) constant ratio designs where drug concentrations are chosen based on an equipotent activity (i.e., the ratio of the IC50s) and serial dilutions are prepared to obtain a dose–effect (or concentration) range for a given ratio (32, 33). A list of methods used to evaluate drug interactions is found in Table 13.2. Clearly, considerable effort has been given to accurately quantify drug:drug synergy; however, this review will describe the methods most commonly employed in the literature.

The most common nonconstant ratio approach to evaluate drug combinations for synergy employs a checkerboard drug combination design. In this method, the drug concentrations and drug ratios are varied. For example, in a 7 × 7 checkerboard layout for a two-drug combination each drug is diluted to generate seven different concentrations. Ideally each individual drug dilution will provide concentrations that provide the full range of tumor cell growth inhibition (e.g., ≤20% to ≥90%). In this design, drug A is diluted vertically and drug B is diluted horizontally in a standard multi-well plate format and combining the two dilution groups results in 49 distinct combinations of the two drugs in addition to the seven concentrations of each individual drug. For most two-drug combinations, basing the dilutions on drug concentrations that span the entire cytotoxicity curve for the individual agents will lead to a rather ad hoc assortment of drug ratios and effective concentrations.

A major disadvantage to the checkerboard approach is the large number of fixed ratios that are evaluated at a limited number of effect levels (concentrations). For example, applying the 7 × 7 matrix design described previously to gemcitabine and cisplatin tested in the A549 non-small cell lung cancer cell line results in

**Table 13.2**  
**Various drug combination interaction methods used for evaluating synergy (adapted from (37))**

Evaluation models	References
Isobologram (1870)	(84, 85)
Loewe additivity (1926)	(86–89)
Bliss independence response surface approach (1939)	(90)
Fractional product method of Webb (1963)	(91)
Multivariate linear logistic model (1970)	(92)
Approach of Gessner (1974)	(93)
Method of Valeriote and Lin (1975)	(94)
Method of Drewinko et al. (1976)	(95)
Interaction index calculation of Berenbaum (1977)	(35)
Method of Steel and Peckman (1979)	(36)
Median-effect method of Chou and Talalay (1984)	(41)
Method of Berenbaum (1985)	(96)
Method of Greco and Lawrence (1988)	(97)
Method of Pritchard and Shipman (1990)	(98–100)
Bivariate spline fitting (Sühnel 1990)	(101)
Models of Greco et al. (1990)	(38, 102, 103)
Models of Weinstein et al. (1990)	(39)

33 different gemcitabine:cisplatin molar ratios spanning a range from 1:5 to 1:100,000 (Table 13.3). Note that drug concentrations were chosen such that each drug spans its own dose–response curve, from low cell growth inhibition to high cell growth inhibition. The IC<sub>50</sub> values for gemcitabine and cisplatin in A549 cells are 0.007 and 4.2  $\mu\text{M}$ , respectively, a difference of approximately 600-fold. At an IC<sub>50</sub> matched ratio (1:600) the nearest ratios evaluated by this checkerboard design are 1:500 and 1:750, indicating that only a few ratios are tested near the steepest and most sensitive region of the dose–response curves (i.e., at the IC<sub>50</sub> value). Further, of the 33 ratios generated, only 8 are evaluated at more than 1 effect level or concentration (gemcitabine:cisplatin ratios of 1:50, 1:100, 1:200, 1:500, 1:1,000, 1:2,000, 1:5,000, and 1:10,000), with the 1:500 ratio being evaluated at a maximum of only 4 effect levels. Therefore, using a conventional checkerboard

**Table 13.3**  
**The gemcitabine and cisplatin ratios obtained when using a checkerboard design in the A549 cell line. The individual drug concentrations were chosen to obtain effect levels that spanned the dose–response curves**

Viability		Cisplatin (IC50 ~ 4.2 $\mu$ M)							
		99%	96.5%	77.5%	51.3%	37.5%	8.3%	3.4%	
Drug Dose		0.1 $\mu$ M	0.5 $\mu$ M	1.0 $\mu$ M	4 $\mu$ M	6 $\mu$ M	10 $\mu$ M	50 $\mu$ M	
Gemcitabine	100%	1:200	1:1,000	1:2,000	1:8,000	1:12,000	1:20,000	1:100,000	
(IC50 ~ 0.007 $\mu$ M)	97.4%	1:100	1:500	1:1,000	1:4,000	1:6,000	1:10,000	1:50,000	
	88.7%	1:50	1:250	1:500	1:2,000	1:3,000	1:5,000	1:25,000	
	66.9%	1:20	1:100	1:200	1:800	1:1,200	1:2,000	1:10,000	
	36.2%	1:12.5	1:62.5	1:125	1:500	1:750	1:1,250	1:6,250	
	29.8%	1:10	1:50	1:100	1:400	1:600	1:1,000	1:5,000	
	20.9% <sup>a</sup>	1:5	1:25	1:50	1:200	1:300	1:500	1:2,500	

<sup>a</sup>Maximum effect was observed at the 0.02  $\mu$ M dose; higher concentrations resulted in no further reduction in cell viability

approach limits the evaluation of the concentration dependency for any particular gemcitabine:cisplatin ratio.

Drug combination schemes where drug:drug ratios are maintained by equivalent dilutions of drug A and drug B in a checkerboard design can be utilized; however, this often results in one of the drugs failing to span the full dose–response curve and the corresponding loss of synergy information in this portion of the dose–response curve. This can be particularly important if missing data occurs at high tumor growth inhibition, considering that for chemotherapeutics to be clinically effective multilog tumor cell kill is required. Thus, the synergy results obtained at high cell kill values are likely to be much more relevant than observations at low effect levels such as an effective dose (ED) of 20% or 30% (ED20 and ED30 reflect concentrations that result in 20% and 30% tumor cell growth inhibition, respectively).

*3.1.1. Fixed Ratio In Vitro Synergy Analysis: Isobologram, Surface Response, and Median-Effect Methods*

In vitro synergy analysis based on fixed drug ratios offers an alternative approach to identifying synergistic drug combinations. The most notable of these are the isobologram, surface response, and median-effect analysis methods, which are described in greater detail below. A constant-ratio approach has the benefit of evaluating the drug combination at a fixed drug:drug ratio over the full range of fraction of affected cells ( $f_a$ ; equivalent to effective dose, ED, the percent tumor growth inhibition relative to control cells) and therefore one can assess whether changes in synergy/antagonism occur for a particular ratio as drug concentrations vary.

Isobolograms (or Isobol) are prepared for each fixed ratio from equally effective dose pairs for a single effect level. It should be noted that if one of the individual dose–response curves do not attain the chosen effect level, an isobol cannot be evaluated at that effect level and a lower effect level must be chosen or higher drug concentrations must be evaluated. Figure 13.1 shows an isobologram for the irinotecan:floxuridine combination adapted from Harasym et al. (34) at an ED75 (effective dose required to achieve 75% tumor cell growth inhibition). The ED75 isobol is generated from the dose of irinotecan required to elicit an ED75 plotted on the  $y$ -axis and the dose of floxuridine required to generate an ED75 plotted on the  $x$ -axis. The straight line joining the two data points on each of the axes is the line of additivity. For experimental combinations the drug concentrations required to generate an ED75 response are then plotted. Data points that lie below the line of additivity are considered synergistic, on the line as additive, and above the line as antagonistic. In this example, five fixed ratios were evaluated at an ED75 and, with the exception of the 10:1 ratio, the four remaining ratios were synergistic. Isobols are simple to generate and are visually easy to interpret; however, the isobols are not readily evaluated statistically and it is

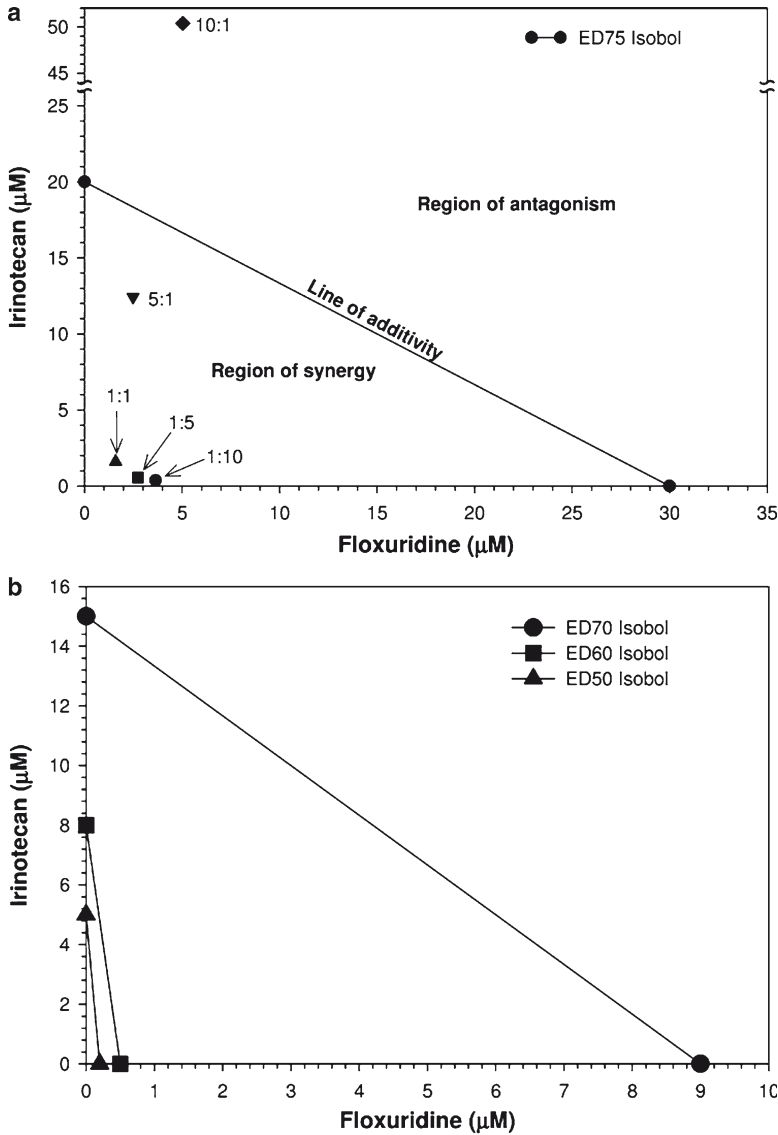


Fig. 13.1. Isobologram of irinotecan and floxuridine in the HCT-116 colorectal cell line (adapted from data presented in [34]). (a) An ED75 isobol including five fixed ratio data points, which were the drug doses of irinotecan:floxuridine required to achieve an ED75. (b) Three isobols are displayed on a single figure, and fixed ratio data are not shown, for clarity.

difficult to quantify the magnitude of the observed synergistic/antagonistic response (i.e., the perpendicular distance from the line of additivity). Although onerous to generate, several modified approaches from the original isobologram methodology do allow for more statistical rigor and provide quantitative measures of synergy (35, 36). Further, when required to evaluate large data sets multiple effect level isobolograms where more than three isobols are plotted (i.e., the simultaneous plots of ED50, ED60,

ED70 isobols on the same figure) become cumbersome and difficult to visualize due to data congestion (Fig. 13.1b). Thus, for large quantities of data, alternative methods that generate similar results are preferred.

Several zero interaction response surfaces (surface response) analysis methods have been described that present data as three-dimensional (3-D) concentration effect curves (37–39). The concentrations of drugs A and B are generally plotted on the  $x$ -axis and  $y$ -axis, and the  $f_a$  (or other observed effect) is plotted on the  $z$ -axis. The 3-D surface that is generated (usually derived from Loewe additivity and/or Bliss independence principles) defines the predicted results of no interaction (zero effect or additivity) for the drug combination.

Zero interaction response surfaces have several advantages including: (1) the evaluation of combinations throughout the complete dose range, (2) analysis when one drug dose is fixed and the second drug dose is varied, and (3) analysis when both drugs are simultaneously varied to keep the dose at a fixed ratio. The latter two points represent cross sections through the zero response surfaces. However, disadvantages of surface response analysis include the need for a large number of regularly dispersed data points, the complexity in implementation, the deficiencies in quantifying the measure of the interaction, and the inability to measure statistical uncertainty (33).

As an example, Fig. 13.2 shows cytarabine and daunorubicin viability data obtained using the CCRF-CEM leukemia cell line plotted in relationship to a zero response surface (CombiTool, IMB-Jena, adapted from data presented in (40)). Data points shown above the surface are synergistic, near the surface indicate zero interaction (additivity), and below the surface are antagonistic. The 5:1 molar ratio of cytarabine:daunorubicin was readily identified as synergistic due to its noticeable separation from the zero interaction surface compared to the other ratios that were either additive or antagonistic. What is most evident from attempting to analyze this type of data format is the difficulty in identifying the synergism, additivity, or antagonism by visual inspection. To analyze the five fixed ratios in the graph visually it is necessary to rotate the graph to inspect under the surface. Further, it is difficult to quantify the extent of synergy (the distance from the zero response surfaces) and the relative response level ( $f_a$ ) at which synergy/antagonism occurred. Therefore, in the analysis of this data set, surface response analysis failed to efficiently identify important quantitative differences in synergy in a manner that is amenable to high data throughput.

Constructing drug combinations for in vitro synergy analysis based on fixed drug ratios has been driven largely by the development of a third method, the median-effect analysis by Chou et al. (33, 41, 42), and this principle has been widely used for combination

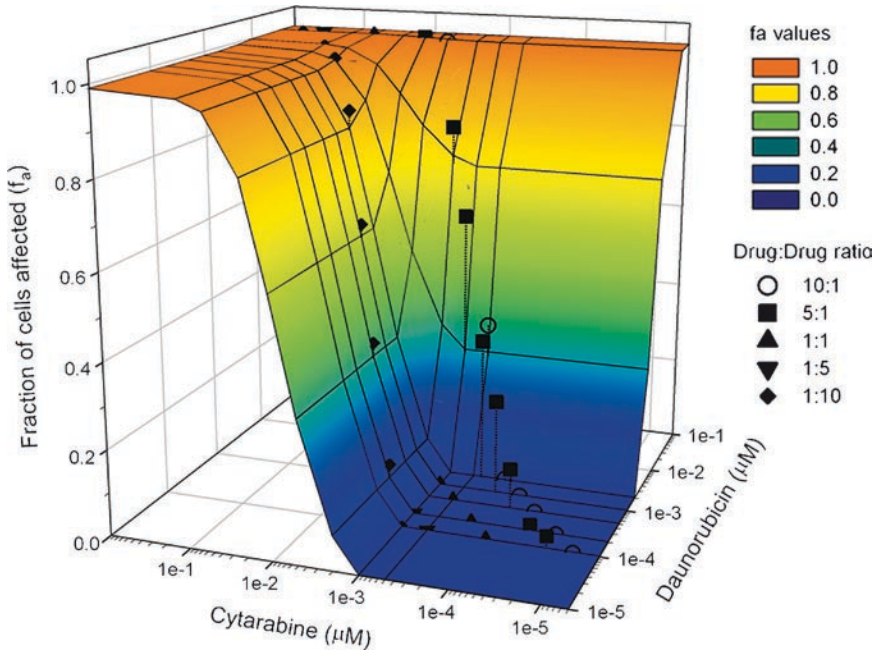


Fig. 13.2. Zero interaction response surfaces (surface response) obtained for cytarabine and daunorubicin in the CCRF-CEM cell line. Data were generated from CombiTool. Data points above the zero interaction surfaces indicate synergy and data points below the surface indicate antagonism (adapted from data presented in (40)).

assessment for numerous years (19, 43–45). In this approach, the ratio of two drugs combined has historically been selected based on their relative  $\text{IC}_{50}$  values, and serial dilutions of this drug combination are prepared to span the entire in vitro dose–response curve. The degree of tumor cell growth inhibition is compared to that for the individual agents across the same concentration range used in the combination. The approach has the benefit of evaluating the combination at a given fixed drug:drug ratio over the full range of fraction of affected cells and therefore one can assess whether changes in drug concentrations affect whether or not a particular drug ratio is synergistic or antagonistic. Although this information is extremely valuable, the drug ratios reflected by  $\text{IC}_{50}$  values of the individual drugs may not reflect those ratios exposed in vivo after systemic administration of a drug combination. Consequently, in order to assess the pharmacological implications of decreasing drug concentrations and changing drug:drug ratios that occur after in vivo administration of conventional drug combinations, multiple ratios must be systematically evaluated in vitro. Historically, this parameter has rarely been investigated in vitro and when it has, the implications of the results obtained with different drug:drug ratios (typically only 2–3) on the in vivo activity of the combination have been unrecognized.

3.1.2. *In Vitro Synergy Analysis Guided by In Vivo Parameters: Combination Index-Fraction Affected Analyses*

The median-effect equation of Chou and Talalay yields identical conclusions for both isobologram and Combination Index (CI)- $f_a$  data (discussed further later) with the advantage of ease of operation, the ability to analyze large data sets, and graphical representations that allow dose-response interpretations. Specifically, where isobolograms are dose oriented, the CI- $f_a$  analyses are effect oriented. Briefly, from dose-response data the median effect (13.1) is log transformed to a linearized equation and thus takes the form of a straight line equation  $y = mx + b$  (13.2).

$$\frac{f_a}{f_u} = \left( \frac{D}{D_m} \right)^m \quad (13.1)$$

$$\log \left( \frac{f_a}{f_u} \right) = m \log(D) - m \log(D_m), \quad (13.2)$$

where  $f_a$  = fraction of cells affected,  $f_u$  = fraction of cells unaffected,  $f_a + f_u = 1$ ,  $D$  = dose of drug,  $D_m$  = the median-effect dose (signifies potency, and is usually near the IC50), and  $m$  = signifies the shape (sigmoidicity) of the dose-effect curve. The latter equation is used to convert monotonic dose-response curves (usually sigmoidal) into straight lines whereby the slope ( $m$ ) and the  $x$ -intercept ( $\log D_m$ ) and hence the  $D_m$  value can be obtained and extrapolated for any dose and effect. Using the Combination Index (CI) (13.3) and using the  $m$  and  $D_m$  values from above the CI value at any effect level ( $f_a$ ) can be determined where:

$$CI = \frac{(D)_1}{(D_x)_1} + \frac{(D)_2}{(D_x)_2}, \quad (13.3)$$

where CI = combination index; CI < 1, = 1, and > 1 indicates synergy, additivity, or antagonism, respectively,  $(D)_1$  and  $(D)_2$  = the drug concentrations in the combination required to inhibit  $X\%$ , and  $(D_x)_1$  and  $(D_x)_2$  = the doses of the individual drugs alone required to inhibit  $X\%$ . It should be noted that the median-effect CI equation is equivalent to the Loewe additivity principle  $I = d_a / D_A + d_b / D_B$  for mutually exclusive agents (33, 37).

The most efficient design for applying the median effect analysis method is to choose a specified fixed ratio as described earlier in the experimental design section, and then perform a series of serial dilutions to obtain a dose-response curve. We use the median-effect equation as our primary method for synergy analysis as it allows for (1) the evaluation of fixed-drug combination ratios at multiple concentrations, (2) the correlation of synergy to the fraction of cells affected, thereby facilitating synergy analysis at high cell kill values, and (3) straightforward generation of synergy

data through the availability of commercially available software (CalcuSyn, BioSoft).

We have utilized the median-effect analysis method to assess the in vitro drug ratio dependency of synergy for several clinically relevant drug combinations (27, 40, 46, 47). Figure 13.3 presents the in vitro synergy results evaluated in this manner for the combination of irinotecan:floxuridine exposed to HCT-116 human colorectal cancer cells (adapted from (34) and (27)). Irinotecan and fluorinated pyrimidine combination therapy are standard of care in metastatic colorectal cancer (48, 49). Taking the traditional approach to analyzing such a combination would result in the generation of a single CI vs.  $f_a$  curve using an irinotecan:floxuridine ratio that would reflect their relative potencies in vitro (10:1 molar ratio in this case; *see* Fig. 13.3a). These data indicate that this drug ratio exhibits significant concentration-dependent synergy since at low  $f_a$  (corresponding to low concentrations of the 10:1 ratio), the combination is nearly additive; however, the combination shifts to strong antagonism when the drug concentration is increased to achieve tumor growth inhibition greater than an  $f_a$  value of 0.5. Higher  $f_a$  values ( $>0.5$ ) are most relevant for cancer applications and under these conditions the 10:1 irinotecan:floxuridine molar ratio was highly antagonistic. Based on these limited data, one could conclude that this combination is, in fact, not desirable from the perspective of drug synergy. However, when four additional drug ratios were evaluated, we observed that other ratios of the same two agents could be identified where strong synergy was obtained over broad drug concentrations reflecting the full range of  $f_a$  values (Fig. 13.3b). Notably, irinotecan:floxuridine ratios of 1:1, 1:5 and 1:10 were synergistic between  $f_a$  values of 0.2 and 0.8. We then compared drug ratio-dependent synergy for the different drug ratios by plotting the CI value as a function of drug ratio for an  $f_a$  value reflecting high cell kill (e.g.,  $f_a=0.8$ ; *see* Fig. 13.3c). These data highlight the fact that as irinotecan:floxuridine concentrations and drug ratios change (as they would following in vivo administration of conventional aqueous-based drug combinations, *see* ref. (34)) conditions would likely occur where the two drugs were exposed at antagonistic drug ratios, and this would compromise therapeutic activity.

### 3.1.3. Automated Screening Methodology

The in vitro evaluations of drug ratio-dependent synergy detailed earlier were performed using five different drug:drug molar ratios ranging from 10:1 to 1:10 in 3–4 cell lines. While this process led to the identification of synergistic drug ratios that could be exploited in vivo via drug delivery systems (*see* later), the intervals between the different drug ratios are relatively large (up to five-fold) and the screening matrix must be tailored to each particular combination in the context of drug concentrations employed.

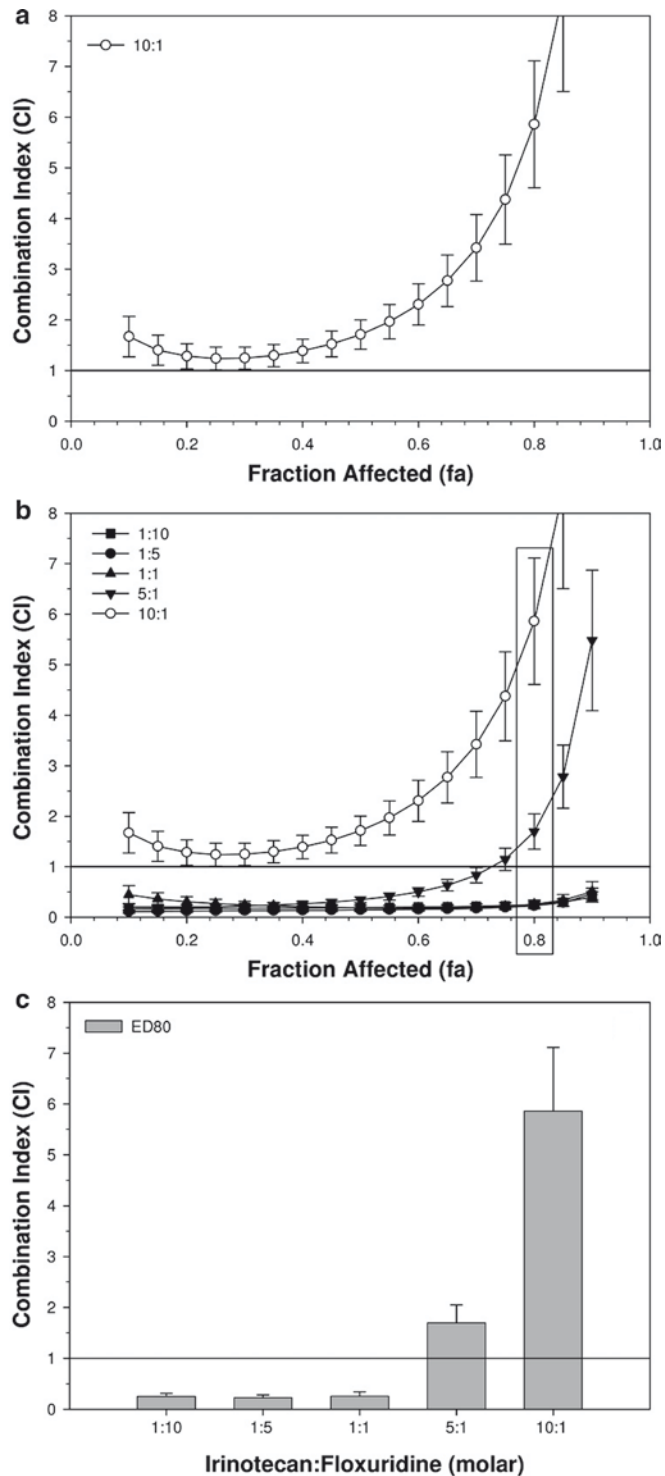


Fig. 13.3. Irinotecan and floxuridine analysis using the median effect principle and combination index (CI) values in the HCT-116 colorectal cell line (adapted from data presented in [34]). (a) CI vs. the fraction affected ( $f_a$ ) at the 10:1 ratio. (b) CI vs.  $f_a$  for five ratios, with the CI values highlighted at the ED80 for each of the five ratios. (c) The indicated CI values from the ED80 for each of the five fixed ratios. CI < 1.0 indicates synergism, CI = 1 indicates additivity, and CI > 1 indicates antagonism.

Manual cell culture procedures are capable of managing the analysis of five fixed ratios plus two individual dose–response profiles using eight serial drug dilutions, triplicate assays, and a minimum of three repeats of each experiment (each experiment represents 630 individual assays). Ideally, however, one would test more drug:drug ratios with smaller intervals in a wider range of tumor cell lines in order to improve the robustness, reliability, and predictability of drug ratio-dependent synergy trends (50–54). Furthermore, a single drug combination matrix would facilitate the application of robotic liquid handling, thereby increasing throughput and allowing virtually any drug combination to be readily examined for in vitro synergy over a wide range of drug ratios and concentrations.

To achieve this goal, we have expanded the number of drug ratios from 5 to 18 where each ratio reflects a twofold increment from its nearest neighbor, have increased the number of concentrations evaluated for each ratio from 8 to 16, have increased the number of experiment repeats from 3 to 4 while maintaining the triplicate replicates within each experiment, and have expanded the number of cell lines screened from 3–4 to 10–20 comprising 5–7 tumor types. In cases where drug combinations are approved for patient use, the in vitro screen is enriched in cell lines representing the clinical indication. The data generated in this process reflect 96,000 individual assays (1,600, 96-well plates). Figure 13.4 presents a schematic illustration of this semiautomated process for systematically evaluating drug combinations for drug ratio-dependent synergy. The process is semiautomated as it relies upon numerous liquid handling robots and workstations (multiplate washers, multiplate readers, etc.) to perform all of the required steps of a cell viability assay. The method evaluates the 18 fixed ratios from a fixed ratio range of 64:1 to 1:2,048. This broad ratio range allows for the collection of fixed-ratio dose–response profiles for drug combinations from agents with similar potencies to those with large differences in potencies (i.e., IC<sub>50</sub> differences of approximately 2,000). The viability assay used is the colorimetric tetrazolium assay, MTT (55); however, with minimal programming and procedural adjustments the methodology can be readily adapted to other colorimetric, fluorescent, or luminescent based assays. The liquid handling robots are used to plate cells into 96-well plates, prepare the required drug master plates plus the required serial dilutions, and to add drugs to the cell containing plates.

The cell viability results generated are entered into a dose–response matrix for each fixed ratio (*see* Fig. 13.4; horizontal rows indicate the 18 fixed ratios and the left most vertical column indicates the cell lines). From the dose–response matrix various data analysis options are available to analyze for combination effects, such as

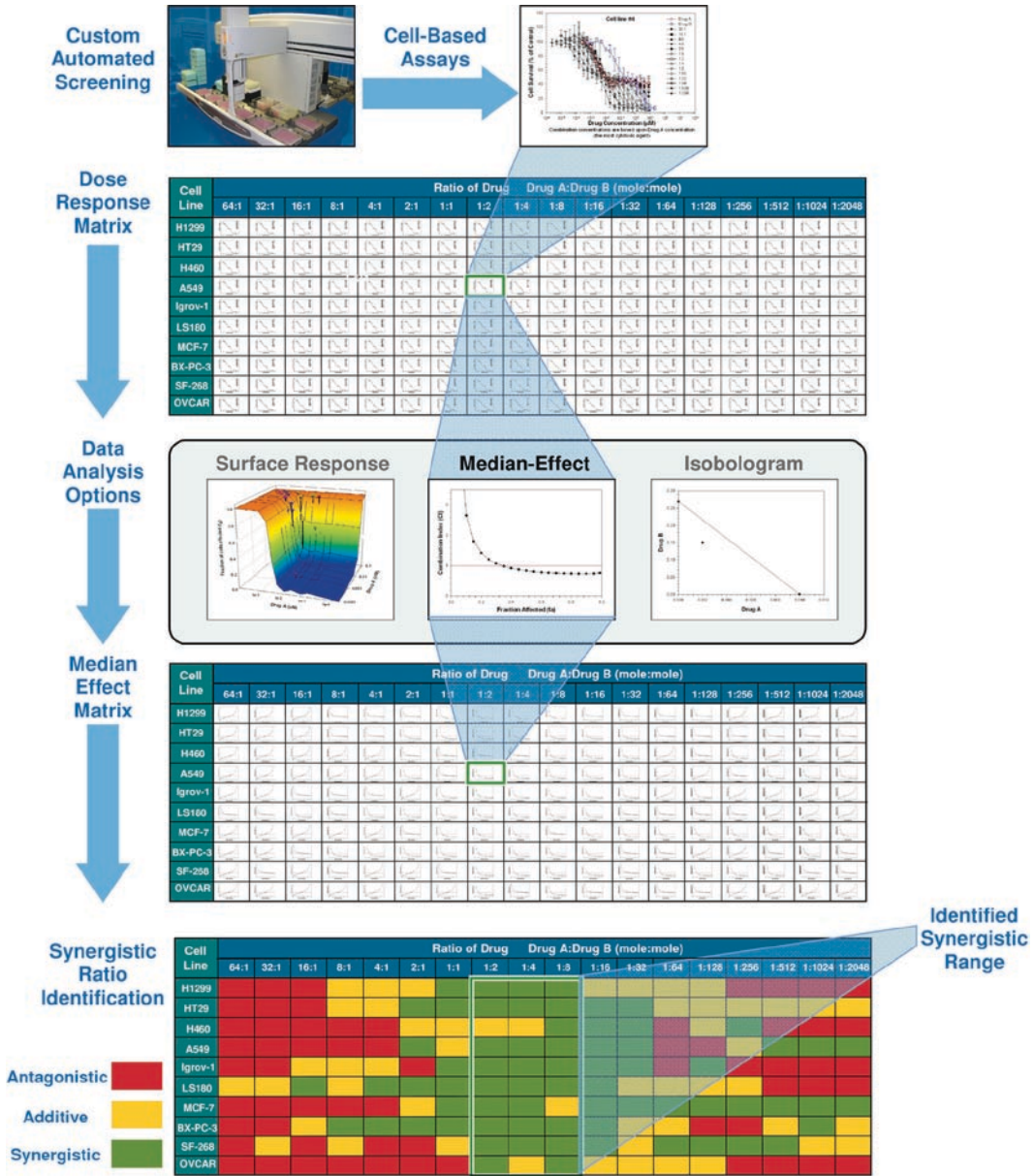


Fig. 13.4. Flow diagram of the in vitro drug screening methodology for the identification of a synergistic fixed-ratio range for a two drug combination in a panel of tumor cell lines.

isobologram, zero interaction (surface response), or median effect. As an example, the median effect analysis leads to the median effect matrix, a summation of data that relates the CI vs.  $f_a$  data sets. Finally, the data are compiled to show the drug combination ratio identification matrix where the combination effect at a defined effect level (i.e., ED80) is displayed. To graphi-

cally highlight the observed pattern of synergism, antagonism, or additive affects the numeric CI values are color coded. CI values between 0 and 0.9 are synergistic (green), values between 0.9 and 1.1 are additive (yellow), and values greater than 1.1 are antagonistic (red). This “ratio heat map” assists in the identification of regions of consistent synergy and antagonism across multiple tumor cell lines at a defined effect level. It should be noted that the broad drug ratio range typically leads to a significant number of data points off the sensitive range of the dose–response curve (e.g., <10% and >90% cell growth inhibition) for given combinations. Consequently, these data points must be “truncated” in order to avoid erroneous skewing of the synergy analysis using the median-effect algorithm.

Table 13.4 presents a “ratio heat map” for the gemcitabine: cisplatin combination. It represents a succinct compilation of the comprehensive data set generated through the automated screening methodology conducted using nine different cell lines and 18 drug ratios. The inclusion of the added cell lines further defines the optimal synergy ratio range near a gemcitabine:cisplatin molar ratio of 1:2, as synergy was observed in all cell lines at this ratio. Higher ratios such as 1:4 for the A2780 ovarian cell line are antagonistic, with widespread drug:drug antagonism observed in several cell lines beyond a drug ratio of 1:128 gemcitabine:cisplatin. Indirectly the tabulated data reveal the different responses of individual cell lines to the gemcitabine:cisplatin combination and such detailed information could be useful for mechanistic correlations. Lastly, the automated screening methodology can be used to generate heat maps for each of the 18 fixed ratios from effect levels of ED5 to high effect levels of ED95 to examine the drug combination effects at any desired effect level. Our primary focus is to identify drug combination synergies at high effect levels (>ED75) and thus at high tumor cell kill. However, this full data set allows synergy to be evaluated at lower effect concentrations, which will be experienced as drugs are eliminated from the body to ensure that significant antagonism does not arise for combinations that may otherwise display synergy at only very high effect levels.

### ***3.2. Translating Drug Ratio-Dependent Synergy In Vivo Using Nanoscale Drug Delivery Systems***

The implication of the drug-dependent antagonism (MDR) revealed by the ratiometric screening results described earlier and elsewhere for other drug combinations (27, 47) is that attention must be given to the concentration and ratio of drug combinations that occur over time after systemic administration in vivo. Basing in vitro synergy testing conditions on pharmacologically relevant drug concentrations and drug ratios observed in vivo may increase our understanding of how conventional drug combinations interact therapeutically. More importantly however, this approach has opened the possibility to exploit drug ratio-dependent synergy

**Table 13.4**  
**A gemcitabine and cisplatin “ratio heat map” displaying the CI values at an ED80 for the standard 18 ratios screened, data from nine cell lines are shown. CI values between 0 and 0.89 are synergistic (green), values between 0.9 and 1.1 are additive (yellow), and values greater than 1.1 are antagonistic (red)**

Cell line Tumor	CI @ ED80																		
	64:1	32:1	16:1	8:1	4:1	2:1	1:1	1:2	1:4	1:8	1:16	1:32	1:64	1:128	1:256	1:512	1:1024	1:2048	
HT-29 Colon	1.80	1.30	4.50	2.30	0.62	0.85	0.69	0.50	0.33	0.16	0.15	0.14	0.03	0.03	0.01	0.02	0.01	0.00	0.00
H1299 Lung	1.70	1.10	3.60	9.70	0.74	0.95	0.40	0.44	0.58	0.44	0.55	0.64	0.18	0.24	0.27	0.54	0.62	0.53	0.53
A549(3) Lung	1.10	0.90	0.85	1.10	0.90	0.85	0.88	0.81	0.55	0.71	0.41	0.51	0.67	1.20	1.90	2.60	3.40	3.80	3.80
A2780 Ovarian	1.30	1.10	0.82	0.96	0.73	0.87	0.76	0.76	1.40	1.20	3.20	8.30	2.90	4.30	3.40	2.30	6.20	5.00	5.00
BxPC-3 Pancreatic	1.30	1.10	0.83	0.52	0.54	0.94	0.68	0.52	0.38	0.23	0.35	0.31	0.48	0.58	1.10	1.10	2.00	0.90	0.90
H460 Lung	1.10	0.88	0.85	1.40	1.20	0.65	0.96	0.82	0.91	1.10	0.67	0.71	1.30	0.76	0.92	0.93	0.86	1.00	1.00
H1299 Lung	9.00	1.70	0.62	0.51	0.49	0.86	0.66	0.62	0.34	0.55	0.49	0.27	0.69	2.50	1.80	4.70	0.63	3.30	3.30
IGROV- Ovarian 1	3.00	0.79	2.90	1.40	1.10	0.70	1.30	0.65	0.87	0.41	0.31	0.57	0.64	1.10	1.20	1.30	1.50	1.20	1.20
MCF-7 Breast	0.80	0.50	1.00	1.10	1.10	1.00	1.00	0.84	0.96	0.81	0.42	0.44	0.39	0.38	0.81	1.30	2.20	2.90	2.90

relationships and avoid drug ratio-dependent MDR antagonism through the use of nanoscale drug delivery systems. This is due to the fact that small (20–200 nm diameter) drug delivery vehicles such as liposomes and nanoparticles do not readily distribute into healthy tissues after systemic administration and can be designed to control the rate at which encapsulated drugs are released from the carrier (56, 57). Consequently, such delivery systems can be constructed to deliver drug combinations in vivo such that the formulated drug:drug ratio can be maintained in the body for extended times after i.v. administration (34, 40, 46, 58, 59). An added advantage of nanoscale particulate carriers is that they display enhanced penetration and retention (EPR) effects in solid tumors due to the associated leaky vasculature and poor lymphatic drainage, which results in selective accumulation of the delivery vehicles and their encapsulated contents in sites of tumor growth (56, 60). The ideal drug vehicle for multiple, synergistic agents must coordinate the pharmacokinetics and biodistribution of both drug agents to ensure delivery of both drugs to the tumor site at the desired synergistic ratio. Dissimilar drug leakage rates or tumor distributions between the two drugs could lead to compromised efficacy via drug ratio-dependent MDR antagonism. Lastly, the drug carrier should have a relatively prolonged plasma half-life compared to the free agents to allow time for the delivery vehicle to extravasate into tumor tissue and exploit the EPR effect for small particulate drug carriers.

Delivery of two agents at a defined ratio through use of a drug delivery vehicle can use one of two strategies. The simplest approach is to formulate each drug component into a separate carrier and combine the two formulated drugs at the desired ratio (Fig. 13.5a). This method has the advantage of facile generation of the desired ratio; however, one must ensure that the drug release rates for both agents are identical and that the biodistribution of both carriers is unaffected by the encapsulation of different agents. These concerns can be eliminated through encapsulation of both active species in a single carrier system (Fig. 13.5b). Such a system presents added complexity to the formulation of a fixed ratio combination agent; iterative variation of internal buffer components and carrier composition is used to coordinate the release of both drugs so that the plasma drug elimination kinetics is matched. For this purpose, liposome technology is better developed than other nanoscale platforms (e.g., nanoparticles, micelles, nanospheres); therefore, the following discussion will focus on development of liposomal carriers.

### 3.2.1. Designing Liposomes to Deliver Fixed-Ratio Drug Combinations

Liposome drug delivery technology has advanced considerably over the past 25 years to the point where there are now several approved liposomal products of single anticancer agents (e.g., DepoCyt (cytarabine), Doxil (doxorubicin), DaunoXome (daunorubicin)). Liposomes are typically formulated with near equimolar amounts of inert, uncharged lipids such as phosphatidylcholine

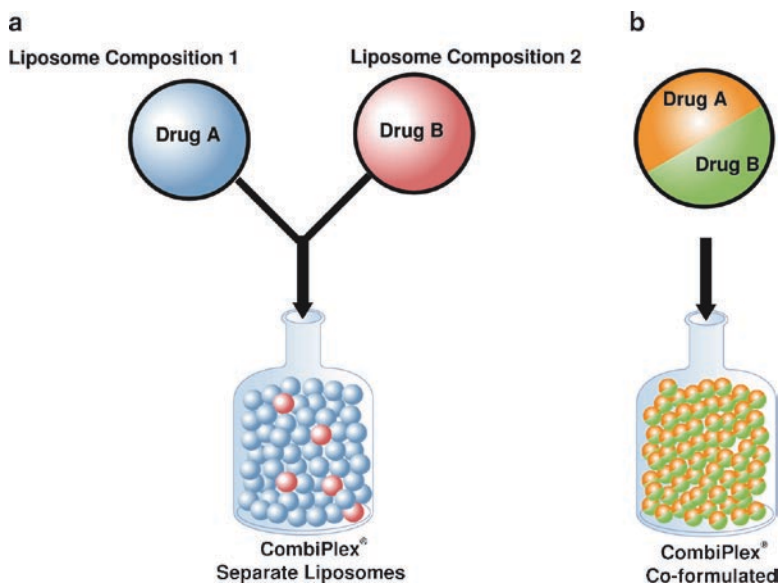


Fig. 13.5. Formulation strategies for encapsulation of two drug species at a fixed drug ratio in vivo. (a) Mixing of two individual encapsulated agents; (b) Coencapsulation of two agents within a single drug vehicle.

and cholesterol. Addition of polyethyleneglycol (PEG) to create PEG-coated “stealth” liposomes (61) or negatively charged lipids (e.g., distearoylphosphatidylglycerol (DSPG) (62)) greatly enhances the plasma circulation time of the liposomes by increasing stability and preventing opsonization by the immune system. The lipid composition also plays a major role in the retention of drugs encapsulated within the liposome (47). The phase transition temperature of saturated lipids increases with acyl chain length (e.g., from C14 to C18) accompanied by a concomitant increase in drug retention properties (62, 63). Cholesterol composition can also be manipulated to tune drug release rates in vivo (64, 65). We have noted that liposomes comprising high phase transition temperature lipids containing relatively low amounts of cholesterol ( $\leq 20\%$  mole ratio) are particularly well suited to coordinated retention of multiple drug agents due to their stable gel phase state in vivo.

Drug encapsulation of liposomes is achieved through either passive or active loading. Passive loading is conducted by extrusion of the liposomes in the presence of the drug (40, 66, 67). Drug loading efficiencies are usually low ( $<10\%$ ) and drug retention can be poor when injected in vivo (66). Active loading is typically highly efficient (drug loading efficiency  $>90\%$ ) and rapid. An appropriate transmembrane gradient (pH, ion, metal) is established that typically causes a chemical or physical change in the drug once encapsulated. As an example, pH gradients typically cause deprotonation or protonation of a weak acid/base moiety of the drug molecule upon encapsulation such that the drug becomes charged

within the liposome and thus far less membrane-permeant after encapsulation (66, 68–70). Other mechanisms related to this concept include intraliposomal drug precipitation (71), metal complexation (72–75), and antiport exchange of drugs and excipients (76).

Development of a coencapsulated liposomal formulation of floxuridine and irinotecan (CPX-1) illustrates the intricate design–function relationships inherent in delivery of fixed ratio chemotherapeutic agents via a drug delivery vehicle (46). Figure 13.6 depicts the release of irinotecan and floxuridine from several liposomal formulations containing different amounts of cholesterol (Chol) in distearoylphosphatidylcholine (DSPC)/distearoylphosphatidylglycerol (DSPG) liposomes. For encapsulated irinotecan (Fig. 13.6a), as the cholesterol component is increased from 0 to 15% mole ratio (of the total lipid), the plasma half-life increases dramatically from less than 2 h for 80:0:20 DSPC:Chol:DSPG to ~15 h for 65:15:20 (DSPC:Chol:DSPG). This sensitivity of irinotecan release to cholesterol is contrasted by the insensitivity of the second drug floxuridine over this cholesterol range (Fig. 13.6b). Floxuridine leakage rates from the four different liposome formulations are virtually independent of liposome cholesterol content between 0 and 20 mole percent cholesterol. In this case, the 70:10:20 DSPC:Chol:DSPG formulation was selected to coencapsulate irinotecan and floxuridine as it coordinated the plasma PK properties of the two active agents.

The internal buffer composition was also instrumental in controlling the drug release properties of CPX-1. The *in vitro* release rate of irinotecan was found to be sensitive to the presence of copper in the internal liposomal buffer of CPX-1, while floxuridine release was largely insensitive to copper. Intensive biophysical characterization of both formulations revealed that the aggregation state of irinotecan was modulated by the encapsulated copper gluconate-triethanolamine buffer system; irinotecan formed higher order aggregates in the absence of copper than led to a slower, uncoordinated release relative to floxuridine (77).

Careful formulation of multiple drug agents to maintain a particular ratio *in vivo* requires iteration of encapsulation techniques to optimize drug encapsulation efficiency, drug retention, and biodistribution properties. The use of *in vivo* data, particularly pharmacokinetic evaluation of plasma clearance rates of both drugs, is essential to guide the formulation process and lock in the desired drug ratio within the carrier. While coformulation of two active agents into drug vehicles is gaining interest in the literature (3, 40, 46, 78–82), attention must be paid to the release properties of both drugs to ensure that the encapsulated drug ratio is not changing over time. Several recent efforts either failed to measure for drug release rates (79, 81, 82) or to maintain the starting drug ratio (72). Use of drug delivery vehicles that successfully coordinate the delivery of the two active agents at a

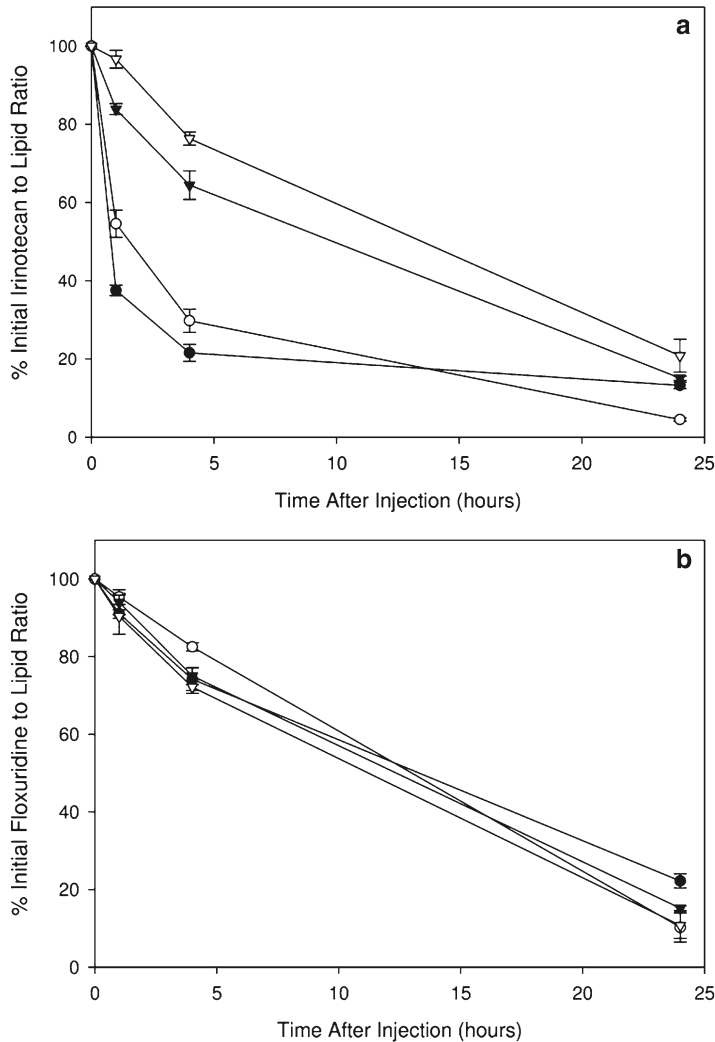


Fig. 13.6. The in vivo retention of irinotecan (a) and floxuridine (b) coformulated in various liposomal formulations. Liposomes composed of DSPC:Chol:DSPG (65:15:20 molar ratio); (*open rectangle*), DSPC:Chol:DSPG (70:10:20 molar ratio); (*filled down triangle*), DSPC:Chol:DSPG (75:5:20 molar ratio); (*open circle*), and DSPC:DSPG (80:20 molar ratio); (*filled circle*) (Reprinted from [46] with permission from Elsevier).

predictable, nonantagonistic ratio is essential to this methodology of mitigating drug ratio-dependent MDR antagonism.

### 3.3. In Vivo Evaluation of Fixed Ratio Combination Therapies

The importance of avoiding exposure of tumor cells to antagonistic drug ratios is elucidated through in vivo comparisons of antitumor activity of the fixed synergistic ratio combination formulation against the combination in which the ratio is uncontrolled (i.e., a free drug cocktail), and most importantly against a fixed liposome-encapsulated antagonistic ratio of the two active species. The goal of such studies is to establish the efficacy superiority of

the fixed synergistic ratio formulation of the two agents by ensuring that (1) a contribution to the observed efficacy is made by both agents and (2) the exposure of tumor cells to a synergistic drug ratio leads to improved efficacy over formulations in which either the ratio is uncontrolled or set within an antagonistic range. Therefore, evaluation of *in vivo* efficacy of fixed-ratio combination agents (e.g., CombiPlex formulations) must include assessment of its efficacy against the free drug cocktail, the singly formulated liposomal agents, and finally against a formulation in which the drug ratio is fixed in a region previously identified as antagonistic.

Typically, mouse models of cancer are employed for this analysis. Prior to formal efficacy experiments, the maximum tolerable doses of each agent are determined, defined as a single dose or series of doses that results in less than 15% of total body weight loss and no toxicity-related mortality for any one dose or schedule of doses. Human xenograft solid tumors subcutaneously grown in immune-compromised mice may be utilized and selected on the basis of defined genetics and growth attributes. Tumor cells utilized in these experiments can be genetically manipulated or selected to express preferable properties and are injected into mice. Once the tumors have grown to a palpable (measurable) size, delivery vehicle and free drug compositions can be administered, preferably intravenously, and their effects on tumor growth are monitored.

It is not readily possible to analyze efficacy data for synergistic or antagonistic interactions by median effect, surface response, or isobologram analysis in an *in vivo* model. Generation of an appropriate (i.e., statistically robust) data set using animal models would require a dose titration of each individual liposomal agent and the combined agents at several ratios and using multiple experimental repeats: clearly the number of animals required for such a study would be prohibitive and the reproducibility between experiments would be far less than for *in vitro* experiments. The efficacy of the synergistic CombiPlex formulation is therefore determined across multiple xenograft tumor models to ensure that the superior *in vitro* efficacy of the synergistic drug ratio translates to *in vivo* efficacy improvements. Secondly, the efficacy of the competing free drug cocktail is optimized by determining the most favorable dose and treatment schedule so that free cocktail *in vivo* efficacy represents the best possible performance of an unrestricted drug ratio formulation. Doses of all agents are then administered at or near MTD to account for differences in therapeutic index. It is worth noting that this frequently requires somewhat lower doses of the combined CombiPlex agent relative to the individual liposomal drugs due to the aggregate toxicity of the combined agents.

Assessment of antitumor activity is most conveniently measured through volume measurement of subcutaneous xenograft tumors or by survival studies for nonsolid tumors. Several methods are available for statistical comparisons between treatment groups. Tumor growth delay ( $T - C$ ) is measured as the median time in days for a treated group ( $T$ ) to reach an arbitrarily determined tumor size (for example, 400 mg) minus median time in days for the control group to reach the same tumor size while tumor regression as a result of treatment may also be used as a means of evaluating a tumor model. Results are expressed as reductions in tumor size (mass) over time. The preferred method of calculated cell kill for solid tumor model evaluation involves measuring tumors repeatedly by calipers until all exceed a predetermined size (e.g., 400 mg). The tumor growth and tumor doubling time can then be evaluated.  $\log_{10}$  cell kill parameters can be calculated by (13.4a–13.4c):

$$\frac{\log_{10}\text{cell kill}}{\text{Dose}} = \frac{(T - C)}{((3.32)(T_d)(\text{No. of doses}))}, \quad (13.4a)$$

$$\log_{10}\text{cell kill (total)} = \frac{(T - C)}{(3.32(T_d))}, \quad (13.4b)$$

$$\log_{10}\text{cell kill (net)} = \frac{((T - C) - (\text{duration of } R_x))}{(3.32(T_d))}, \quad (13.4c)$$

where  $(T - C)$  = tumor growth delay,  $T_d$  = Tumor doubling time. Evaluation of nonsolid tumors include measurement of increase in life-span (ILS%), tumor growth delay ( $T - C$ , as above) or long-term survivors (cures). Increase in lifespan is calculated by dividing the median survival time of the treatment group by the median survival time of the control group. Long-term survivors are identified as subjects that survive up to and beyond three times the survival of the untreated group.

The efficacy advantages of the CombiPlex platform to avoid exposure of tumors to antagonistic drug ratios that may lead to MDR are exhibited in Figs. 13.7 and 13.8. The CombiPlex formulation CPX-1, a liposomal formulation of irinotecan and floxuridine coencapsulated at the synergistic ratio of 1:1, was evaluated for antitumor activity (cell line: pancreatic Capan-1) against the free drug cocktail, the individual liposomal components, and a second coencapsulated formulation of irinotecan and floxuridine at an antagonistic ratio of 1:10 (Fig. 13.7, adapted from data presented in (27)). CPX-1, at a dose of 37  $\mu\text{mol/kg}$  of each agent, showed superior efficacy over all other groups with a calculated log cell kill (LCK) value of 1.8, besting the LCK efficacy of

high-dose liposomal irinotecan (37  $\mu\text{mol}/\text{kg}$ ) of 1.4 by nearly 2.5 times, and the LCK of liposomal floxuridine (37  $\mu\text{mol}/\text{kg}$ ) of 0.3 by  $\sim 62$  times. CPX-1 is also clearly superior to both free drugs dosed at their MTD; irinotecan (148  $\mu\text{mol}/\text{kg}$ ) and floxuridine (1,000  $\mu\text{mol}/\text{kg}$ ) achieved LCK values of only 0.6 and 0.4, respectively. A 1:1 free drug cocktail formulation of irinotecan and floxuridine (148:148  $\mu\text{mol}/\text{kg}$ ) was also inferior (LCK value 0.65, a factor of 14 times less than CPX-1), demonstrating the value of encapsulating drug-ratio dependent agents in a drug delivery vehicle that controls drug ratios. Finally, encapsulation of antagonistic drug ratios led to decreased efficacy despite the addition of more drug. A dose of liposomal irinotecan at 7.4  $\mu\text{mol}/\text{kg}$  led to an observed LCK of 1.1, while liposomal irinotecan:floxuridine at a dose of 7.4:74  $\mu\text{mol}/\text{kg}$  had an LCK of 0.55, nearly 3.6 times less activity despite an identical dose of irinotecan and addition of 74  $\mu\text{mol}/\text{kg}$  of floxuridine. This result clearly demonstrates the deleterious effects on *in vivo* efficacy that occur when tumors are exposed to cytotoxic drugs at an antagonistic ratio (27). Later tumor distribution studies confirmed that the augmented activity of CPX-1 and decreased activity of the 1:10 irinotecan:floxuridine formulation was due to synergistic and antagonistic drug interactions at the tumor site, as both formulations delivered the two drugs at their respective ratios to the solid tumors (34).

The drug ratio-dependent antitumor activity of a liposomal formulations of cytarabine:daunorubicin (CPX-351) was demonstrated in P388 ascites tumor-bearing BDF-1 mice (40). The 55-day survival percentages of several liposomal formulations of the two drugs are shown in Fig. 13.8. The highest survival percentage of 100% was observed for the 5:1 ratio of cytarabine and daunorubicin, previously demonstrated to be synergistic *in vitro*. Survivors steadily decreased for all other formulations, dropping to 83% for a 12:1 ratio formulation (despite 50% more cytarabine and only 25% less daunorubicin), and, strikingly, only 50% survival for a 3:1 cytarabine:daunorubicin formulation that actually administered the same amount of cytarabine (10  $\mu\text{mol}/\text{kg}$ ) as CPX-351, but nearly twofold more daunorubicin (7.4  $\mu\text{mol}/\text{kg}$  for the 3:1 formulation vs. 4  $\mu\text{mol}/\text{kg}$  for CPX-351). In this instance, more drug actually led to less activity, despite tumor biodistribution studies demonstrating drug delivery at the established ratios in both cases. Clearly, deviation from synergistic ratio toward ratios known to be antagonistic can lead to compromised efficacy.

Further translation of *in vitro* drug screening informatics to *in vivo* efficacy is provided by a study by Abraham et al. (72). Previous *in vitro* cytotoxicity studies had demonstrated that coadministration of doxorubicin and vincristine was antagonistic, although detailed studies to identify drug ratio regions of synergy/

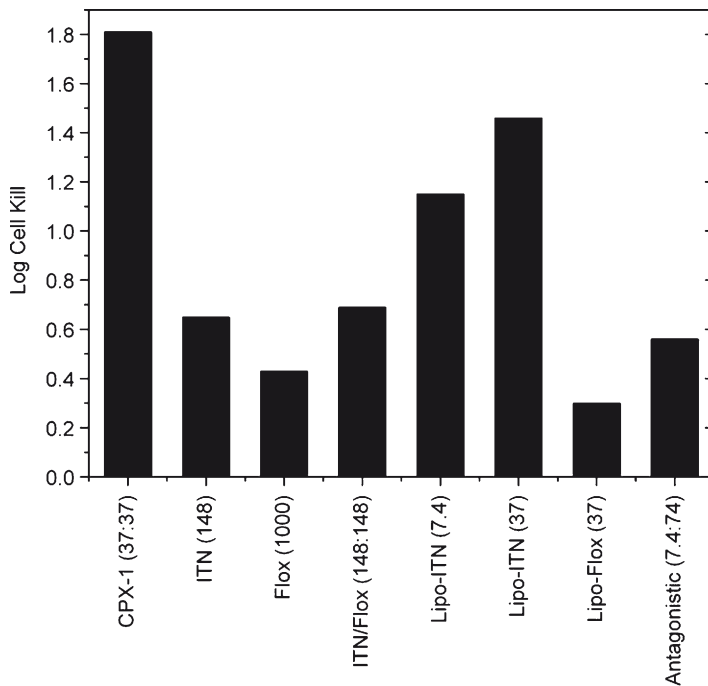


Fig. 13.7. Quantitative analysis of CPX-1 in vivo activity against Capan-1 pancreatic xenograft tumor model (adapted from data presented in [27]). Numbers in brackets represent dose of irinotecan:floxuridine or single agents in  $\mu\text{mol/kg}$ . CPX-1 liposomal formulation of irinotecan:floxuridine at synergistic 1:1 molar ratio, ITN irinotecan, Flox floxuridine, Lipo liposomal, antagonistic liposomal formulation of irinotecan:floxuridine at antagonistic 1:10 molar ratio.

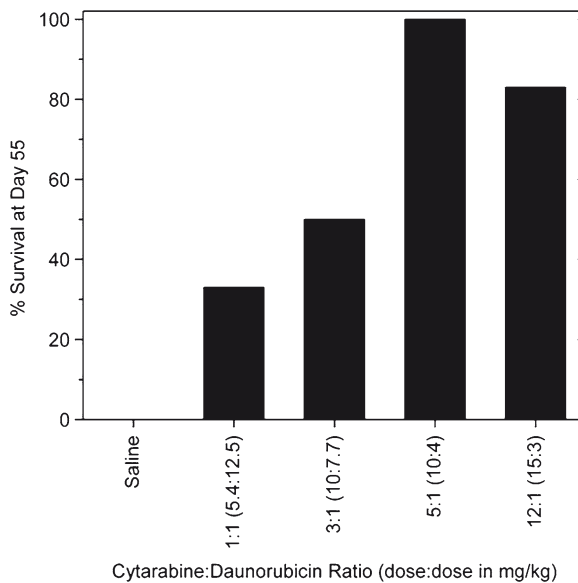


Fig. 13.8. Survival of BDF-1 mice bearing P388 ascites tumors at day 55 following Q3Dx3 treatment with saline or coencapsulated liposomal cytarabine:daunorubicin at different drug:drug ratios (adapted from data presented in (40)).

antagonism were absent. Drug:drug antagonism was confirmed in subsequent *in vivo* efficacy studies, which demonstrated equivalent efficacy for liposomal doxorubicin:vincristine vs. the single agent of liposomal doxorubicin. This result agreed with an earlier report of antitumor efficacy of liposomal vincristine coadministered with the liposomal doxorubicin agent Doxil. In this study the efficacy of the combined agents was actually less than that observed for Doxil alone, despite the efficacy of both individual liposomal agents being superior to the free drug (83). In both cases, it should be noted that exquisite *in vivo* control of drug ratios was lacking: in the former case; the plasma drug:drug ratio changed from the initial 4:1 vincristine:doxorubicin ratio to over 20:1 in 24 h (72) while the pharmacokinetic differences between the individual liposomal formulations of vincristine and doxorubicin were not examined. These studies, while examples of incomplete consideration of drug ratio analysis, demonstrate the translation of *in vitro* antagonism leading to compromised *in vivo* efficacy likely due to a drug ratio-dependent MDR mechanism.

---

#### 4. Conclusion

MDR continues to be a significant impediment to improving the outcomes of cancer patients to chemotherapy treatment. Current combination therapies, while typically more effective than single agent treatments, can be subject to a newly identified form of MDR that manifests itself as a resistance to drugs presented at discrete ratios and concentrations when administered concurrently. In the current treatment paradigm, multiple agents are administered in saline-based cocktail that cannot account for the disparate pharmacokinetics of each individual agent, which generally leads to rapidly and widely changing drug ratios postadministration. Therefore, plasma elimination of free drug cocktails can result in tumor exposure to antagonistic drug ratios and corresponding compromised efficacy. In this review, we have detailed methods by which this drug-ratio dependent MDR mechanism can be identified and bypassed, resulting in improved antitumor efficacy.

Screening for ratio-dependent drug interactions is best achieved through an approach that assesses drug interactions across a wide range of drug ratios and effect levels. Using these techniques has led to identification of drug ratio-dependent synergistic and antagonistic interactions for numerous drug combinations. Given the apparent broad applicability of drug ratio-dependent synergy and the ability to exploit such information

in vivo by delivering fixed drug ratios in particulate drug carriers, we have demonstrated the application of automated, ratiometric drug combination screening in order to facilitate the systematic evaluation of multiple drug combinations at numerous ratios under pharmacologically relevant conditions with high throughput. Liposomal- and nanoparticle-based delivery technologies can be developed to deliver synergistic drug combinations at fixed drug ratios and avoid tumor exposure to antagonistic ratios. Codelivery and coordinated release of synergistic drug combinations facilitate the achievement of maximum efficacy by maintaining synergy throughout the pharmacodynamic (dose–response cytotoxicity) profile and avoidance of antagonistic ratios in vivo.

## References

1. Frei EI, Freireich EJ (1964) Leukemia. *Sci Am* 210:88–96
2. Freireich EJ, Frei EI (1964) Recent advances in acute leukemia. *Prog Hematol* 27:187–202
3. Ramsay EC, Dos Santos N, Dragowska WH, Laskin JJ, Bally MB (2005) The formulation of lipid-based nanotechnologies for the delivery of fixed dose anticancer drug combination. *Curr Drug Del* 2:341–351
4. Ewesuedo RB, Ratain MJ (2003) Principles of cancer therapeutics. In: Vokes EE, Golomb HM (eds) *Oncologic therapies*. Springer, Secaucus, NJ, pp 19–66
5. Shabbits JA, Krishna R, Mayer LD (2001) Molecular and pharmacological strategies to overcome multidrug resistance. *Expert Rev Anticancer Ther* 1:89–98
6. Coley HM (2008) Mechanisms and strategies to overcome chemotherapy resistance in metastatic breast cancer. *Cancer Treat Rev* 34:378–390
7. Shabbits JA, Hu Y, Mayer LD (2003) Tumor chemosensitization strategies based on apoptosis manipulations. *Mol Cancer Ther* 2: 805–813
8. Zhou SF, Wang LL, Di YM et al (2008) Substrates and inhibitors of human multidrug resistance associated proteins and the implications in drug development. *Curr Med Chem* 15:1981–2039
9. Perez-Tomas R (2006) Multidrug resistance: retrospect and prospects in anti-cancer drug treatment. *Curr Med Chem* 13:1859–1876
10. Nobili S, Landini I, Gigliani B, Mini E (2006) Pharmacological strategies for overcoming multidrug resistance. *Curr Drug Targets* 7:861–879
11. Shah MA, Schwartz GK (2001) Cell cycle-mediated drug resistance: an emerging concept in cancer therapy. *Clin Cancer Res* 7:2168–2181
12. Dancy JE, Chen HX (2006) Strategies for optimizing combinations of molecularly targeted anticancer agents. *Nat Rev Drug Disc* 5:649–659
13. Keith CT, Borisy AA, Stockwell BR (2005) Multicomponent therapeutics for networked systems. *Nat Rev Drug Disc* 4:1–8
14. Lehar J, Zimmermann GR, Krueger AS et al (2007) Chemical combination effects predict connectivity in biological systems. *Mol Sys Biol* 3:1–14
15. Cohen MH, Gootenberg J, Keegan P, Pazdur R (2007) FDA drug approval summary: Bevacizumab (Avastin<sup>®</sup>) plus carboplatin and paclitaxel as first-line treatment of advanced/metastatic recurrent nonsquamous non-small cell lung cancer. *Oncologist* 12:713–718
16. Schwartz RN, Vozniak M (2008) Current and emerging treatments in multiple myeloma. *J Manag Care Pharm* 14:S12–S18
17. Tannock IF, de Wit R, Berry WR et al (2004) Docetaxel plus prednisone or mitoxantrone plus prednisone for advanced prostate cancer. *N Engl J Med* 351:1502–1512
18. von der Maase H, Hansen SW, Roberts JT et al (2000) Gemcitabine and cisplatin versus methotrexate, vinblastine, doxorubicin, and cisplatin in advanced or metastatic bladder cancer: results of a large, randomized, multinational, multicenter, phase III study. *J Clin Oncol* 18:3068–3077
19. Hongrapipat J, Kopeckova P, Liu J, Prakongpan S, Kopecek J (2008) Combination chemotherapy and photodynamic therapy with Fab' fragment targeted HPMA copolymer conjugates in human ovarian carcinoma cells. *Mol Pharm* 5:696–709
20. Photiou A, Shah P, Leong LK, Moss J, Retsas S (1997) In vitro synergy of paclitaxel (Taxol) and

- vinorelbine (Navelbine) against human melanoma cell lines. *Eur J Cancer* 33:463–470
21. Frei EI (1972) Combination cancer therapy: Presidential address. *Cancer Res* 32:2593–2607
  22. Adams DJ, Sandvold ML, Myhren F et al (2008) Anti proliferative activity of ELACY (CP-4055) in combination with cloretazine (VNP40101M), idarubicin, gemcitabine, irinotecan and topotecan in human leukemia and lymphoma cells. *Leuk Lymph* 49:786–797
  23. Saiman L (2007) Clinical utility of synergy testing for multidrug-resistant *Pseudomonas aeruginosa* isolated from patients with cystic fibrosis: “the motion for”. *Paediatr Respir Rev* 8:249–255
  24. Seydel JK, Schaper KJ, Rüscher-Gerdes S (1994) Experimental drugs and combination therapy. *Immunobiology* 191:569–577
  25. Timukaynak F, Can F, Azap OK et al (2006) In vitro activities of non-traditional antimicrobials alone or in combination against multidrug-resistant strains of *Pseudomonas aeruginosa* and *Acinetobacter baumannii* isolated from intensive care units. *Int J Antimicrob Agents* 27:224–228
  26. Urban C, Segal-Maurer S, Rahal JJ (2003) Considerations in control and treatment of nosocomial infections due to multidrug-resistant *Acinetobacter baumannii*. *Clin Infect Dis* 36:1268–1274
  27. Mayer LD, Harasym TO, Tardi PG et al (2006) Ratiometric dosing of anticancer drug combinations: controlling drug ratios after systemic administration regulates therapeutic activity in tumor-bearing mice. *Mol Cancer Ther* 5:1854–1863
  28. Mayer LD, Janoff AS (2007) Optimizing combination chemotherapy by controlling drug ratios. *Mol Interv* 7:216–223
  29. Borisy AA, Elliot PJ, Hurst NW et al (2003) Systematic discovery of multicomponent therapeutics. *Proc Natl Acad Sci USA* 100:7977–7982
  30. Kanzawa F, Koizumi F, Koh Y et al (2001) In vitro synergistic interactions between the cisplatin analogue nedaplatin and the DNA topoisomerase I inhibitor irinotecan and the mechanism of this interaction. *Clin Cancer Res* 7:202–209
  31. Raitanen M, Rantanen V, Kulmala J et al (2002) Supra-additive effect with concurrent paclitaxel and cisplatin in vulvar squamous cell carcinoma in vitro. *Int J Cancer* 100:238–243
  32. Mercalli A, Sordi V, Formicola R et al (2007) A preclinical evaluation of pemetrexed and irinotecan combination as second-line chemotherapy in pancreatic cancer. *Br J Cancer* 96:1358–1367
  33. Chou TC (2006) Theoretical basis, experimental design, and computerized simulation of synergism and antagonism in drug combination studies. *Pharmacol Rev* 58:621–681
  34. Harasym TO, Tardi PG, Harasym NL et al (2007) Increased preclinical efficacy of irinotecan and floxuridine coencapsulated inside liposomes is associated with tumor delivery of synergistic drug ratios. *Oncol Res* 16:361–374
  35. Berenbaum MC (1977) Synergy, additivism and antagonism in immunosuppression. *Clin Exp Immunol* 28:1–18
  36. Steel GG, Peckham MJ (1979) Exploitable mechanisms in combined radiotherapy-chemotherapy: the concept of additivity. *Int J Radiat Oncol Biol Phys* 5:85–91
  37. Greco WR, Bravo G, Parsons JC (1995) The search for synergy: a critical review from a response surface perspective. *Pharmacol Rev* 47:331–385
  38. Greco WR, Park HS, Rustum YM (1990) An application of a new approach for the quantitation of drug synergism to the combination of cis-diamminedichloroplatinum and 1- $\beta$ -D-arabinofuranosylcytosine. *Cancer Res* 50:5318–5327
  39. Weinstein JL, Bunow B, Weislow OS et al (1990) Synergistic drug combinations in AIDS therapy. *Ann N Y Acad Sci* 616:367–384
  40. Tardi PG, Johnstone SA, Harasym NL et al (2009) In vivo maintenance of synergistic cytarabine:daunorubicin ratios greatly enhances therapeutic efficacy. *Leuk Res* 33:129–139
  41. Chou TC, Talalay P (1984) Quantitative analysis of dose-effect relationships: the combined effects of multiple drugs or enzyme inhibitors. *Adv Enzyme Regul* 22:27–55
  42. Chou TC (1991) The median-effect principle and the combination index for quantitation of synergism and antagonism. In: Chou TC, Rideout DC (eds) *Synergism and antagonism in chemotherapy*. Academic, New York, pp 61–102
  43. Konecny G, Untch M, Slamon DJ et al (2001) Drug interactions and cytotoxic effects of paclitaxel in combination with carboplatin, epirubicin or vinorelbine in breast cancer cell lines and tumor samples. *Breast Cancer Res Tr* 67:223–233
  44. Lisztwan J, Pornon A, Chen B, Chen S, Evans DB (2008) The aromatase inhibitor letrozole and inhibitors of insulin-like growth factor I receptor synergistically induce apoptosis in

- in vitro models of estrogen-dependent breast cancer. *Breast Cancer Res* 10:R56
45. Saigal B, Glisson BS, Johnson FM (2008) Dose-dependent and sequence-dependent cytotoxicity of erlotinib and docetaxel in head and neck squamous cell carcinoma. *Anticancer Drugs* 19:465–477
  46. Tardi PG, Gallagher RG, Johnstone SA et al (2007) Coencapsulation of irinotecan and floxuridine into low cholesterol-containing liposomes that coordinate drug release in vivo. *Biochim Biophys Acta* 1768: 678–687
  47. Harasym TO, Tardi PG, Johnstone SA et al (2007) Fixed drug ratio liposome formulations of combination cancer therapeutics. In: Gregoriadis G (ed) *Liposome technology volume III: interactions of liposomes with biological milieu*, 3rd edn. Informa Healthcare USA Inc., New York, pp 25–46
  48. Douillard JY, Cunningham D, Roth AD et al (2000) Irinotecan combined with fluorouracil compared with fluorouracil alone as first-line treatment for metastatic colorectal cancer: a multicenter randomised trial. *Lancet* 355:1041–1047
  49. Saltz LB, Cox JV, Blanke C et al (2000) Irinotecan plus fluorouracil and leucovorin for metastatic colorectal cancer. *N Engl J Med* 343:905–914
  50. Corbett T, Valeriote F, LoRusso P, et al (1997) In vivo methods for screening and preclinical testing – use of rodent solid tumors for drug delivery. In: *Anticancer drug development guide: preclinical screening, clinical trials, and approval*, Humana, Totawa, NJ, pp. 75–99
  51. Grindley GB (1982) Multiple models of utility for the rational development of new concepts involved in metabolic modulation. In: Fidler IJ, White RJ (eds) *Design of models for testing cancer therapeutic agents*. Van Nostrand Reinhold, New York, pp 206–214
  52. Harrison S (2002) Perspective on the history of tumor models. In: Teicher BA (ed) *Tumor models in cancer research*. Humana, Totawa, NJ, pp 3–22
  53. Johnson RK (1990) Screening methods in antineoplastic drug discovery. *J Natl Cancer Inst* 82:1082–1083
  54. Kaufmann SH, Peereboom CA, Buckwalter CA et al (1996) Cytotoxic effects of Topotecan combined with various anticancer agents in human cancer lines. *J Natl Cancer Inst* 88: 734–741
  55. Mosmann T (1983) Rapid colorimetric assay for cellular growth and survival: application to proliferation and cytotoxicity assays. *J Immunol Methods* 65:55–63
  56. Maeda H (2001) The enhanced permeability and retention (EPR) effect in tumor vasculature: the key role of tumor-selective macromolecular drug targeting. *Adv Enzyme Regul* 41:189–207
  57. Torchilin VP (2007) Targeted pharmaceutical nanocarriers for cancer therapy. *AAPS J* 9:E128–E147
  58. Batist G, Chi K, Miller W et al (2006) Phase I study of CPX-1, a fixed ratio formulation of irinotecan (IRI) and floxuridine (FLOX), in patients with advanced solid tumors. *J Clin Oncol* 24:2014
  59. Batist G, Miller W, Mayer L et al (2007) Ratiometric dosing of irinotecan (IRI) and floxuridine (FLOX) in a phase I trial: a new approach for enhancing the activity of combination chemotherapy. *J Clin Oncol* 25:2549
  60. Maeda H, Wu J, Sawa T, Matsumura Y, Hori K (2000) Tumor vascular permeability and the EPR effect in macromolecular therapeutics: a review. *J Control Release* 65:271–284
  61. Lasic DD, Martin FJ (1995) *Stealth liposomes*. CRC, Boca Raton, FL
  62. Tari A, Huang L (1989) Structure and function of phosphatidylglycerol in the stabilization of the phosphatidylethanolamine bilayer. *Biochemistry* 28:7708–7712
  63. Boman NL, Mayer LD, Cullis PR (1993) Optimization of the retention properties of vincristine in liposomal systems. *Biochim Biophys Acta* 1152:253–258
  64. Dos Santos N, Mayer LD, Abraham SA et al (2002) Improved retention of idarubicin after intravenous injection obtained for cholesterol-free liposomes. *Biochim Biophys Acta* 1561:188–201
  65. Dos Santos, N., Waterhouse, D., Masin, D. et al (2005) Substantial increases in idarubicin plasma concentration by liposome encapsulation mediates improved antitumor activity. *J Control Release* 105:89–109
  66. Mayer LD, Cullis PR, Bally MB (1994) The use of transmembrane pH gradient-driven drug encapsulation in the pharmacodynamic evaluation of liposomal doxorubicin. *J Liposome Res* 4:529–553
  67. Peleg-Shulman T, Gibson D, Cohen R, Abraham R, Barenholz Y (2001) Characterization of sterically stabilized cisplatin liposomes by nuclear magnetic resonance. *Biochim Biophys Acta* 1510:894–902
  68. Cullis PR, Hope MJ, Bally MB et al (1997) Influence of pH gradients on the transbilayer transport of drugs, lipids, peptides, and metal

- ions into large unilamellar vesicles. *Biochim Biophys Acta* 1331:187–211
69. Drummond DC, Noble CO, Hayes ME, Park JW, Kirpotin DB (2008) Pharmacokinetics and in vivo drug release rates in liposomal nanocarrier development. *J Pharm Sci* 97:4696–4740
  70. Haran G, Cohen R, Bar LK, Barenholz Y (1993) Transmembrane ammonium sulfate gradients in liposome produce efficient and stable entrapment of amphipathic weak bases. *Biochim Biophys Acta* 1151:201–215
  71. Kirpotin DB (2000) Compound loaded liposomes and methods for their preparation. US Patent 6, 110, 491
  72. Abraham SA, McKenzie C, Masin D et al (2004) In vitro and in vivo characterization of doxorubicin and vincristine coencapsulated within liposomes through use of transition metal ion complexation and pH gradient loading. *Clin Cancer Res* 10:728–738
  73. Li C, Cui J, Li Y et al (2008) Copper ion-mediated liposomal encapsulation of mitoxantrone: the role of anions in drug loading, retention and release. *Eur J Pharm Sci* 34:333–344
  74. Ramsay EC, Alnajim J, Taggar A et al (2006) Transition metal-mediated liposomal encapsulation of irinotecan (CPT-11) stabilizes the drug in the therapeutically active lactone conformation. *Pharm Res* 23:2799–2808
  75. Taggar A, Alnajim J, Anantha M et al (2006) Copper-topotecan complexation mediates drug accumulation into liposomes. *J Control Release* 114:78–88
  76. Dicko A, Tardi PG, Xie X, Mayer LD (2007) Role of copper gluconate/triethanolamine in irinotecan encapsulation inside the liposomes. *Int J Pharm* 337:219–228
  77. Dicko A, Frazier AA, Liboiron BD et al (2008) Intra and inter-molecular interactions dictate the aggregation state of irinotecan co-encapsulated with floxuridine inside liposomes. *Pharm Res* 25:1702–1713
  78. Liu Y, Lu W-L, Guo J et al (2008) A potential target associated with both cancer and cancer stem cells: a combination therapy for eradication of breast cancer using vinorelbine stealthy liposomes plus parthenolide stealthy liposomes. *J Control Release* 129:18–25
  79. Wang J, Goh B, Lu W et al (2005) In vitro cytotoxicity of stealth liposomes co-encapsulating doxorubicin and verapamil on doxorubicin-resistant tumour cells. *Biol Pharm Bull* 28:822–828
  80. Webb MS, Johnstone S, Morris TJ et al (2007) In vitro and in vivo characterization of a combination chemotherapy formulation consisting of vinorelbine and phosphatidylserine. *Eur J Pharm Biopharm* 65:289–299
  81. Wu J, Lu Y, Lee A et al (2007) Reversal of multidrug resistance by transferrin-conjugated liposomes co-encapsulating doxorubicin and verapamil. *J Pharm Pharmaceut Sci* 10:350–357
  82. Zhao X, Wu J, Muthusamy N, Byrd JC, Lee RJ (2008) Liposomal coencapsulated fludarabine and mitoxantrone for lymphoproliferative disorder treatment. *J Pharm Sci* 97:1508–1518
  83. Vaage J, Donovan D, Mayhew E, Uster P, Woodle M (1993) Therapy of mouse mammary carcinomas with vincristine and doxorubicin encapsulated in sterically stabilized liposomes. *Int J Cancer* 54:959–964
  84. Fraser TR (1870–1871) An experimental research on the antagonism between the actions of physostigma and atropia. *Proc R Soc Edinb* 7:506–511
  85. Fraser TR (1871) The antagonism between the actions of active substances. *Br Med J* 2:485–487
  86. Loewe S (1928) Die Quantitation Probleme der Pharmakologie. *Ergeb Physiol Biol Chem Exp Pharmacol* 27:47–187
  87. Loewe S (1953) The problem of synergism and antagonism of combined drugs. *Arzneim Forsch* 3:285–290
  88. Loewe S (1957) Antagonism and antagonists. *Pharmacol Rev* 9:237–242
  89. Loewe S, Muischnek H (1926) Effect of combinations: mathematical basis of problem. *Arch Exp Pathol Pharmacol* 114:313–326
  90. Bliss CI (1939) The toxicity of poisons applied jointly. *Ann Appl Biol* 26:585–615
  91. Webb JL (1963) Effect of more than one inhibitor. In: Webb JL (ed) *Enzymes and metabolic inhibitors*, Vol. 1. Academic, New York, pp. 66–79, 487–512
  92. Cox DR (1970) *The analysis of binary data*. Methuen, London
  93. Gessner PK (1974) The isobolographic method applied to drug interactions. In: Morselli PL, Garattini S, Cohen SN (eds) *Drug interactions*. Raven, New York, pp 349–362
  94. Valeriote F, Lin H (1975) Synergistic interaction of anticancer agents: a cellular perspective. *Cancer Chemother Rep* 59:895–900
  95. Drewinko B, Loo TL, Brown B, Gottlieb JA, Freireich EJ (1976) Combination chemotherapy in vitro with adriamycin. Observations of additive, antagonistic, and synergistic effects when used in two-drug combinations on cultured human lymphoma cells. *Cancer Biochem Biophys* 1:187–195

96. Berenbaum MC (1985) The expected effect of a combination of agents: the general solution. *J Theor Biol* 114:413–431
97. Greco WR, Lawrence DL (1988) Assessment of the degree of drug interaction where the response variable is discrete. *Am Stat Assoc, Proc Biopharm Sect* 183–188
98. Prichard MN, Shipman C Jr (1990) A three dimensional model to analyze drug–drug interactions (review). *Antiviral Res* 14:181–206
99. Prichard MN, Shipman C Jr (1992) Response to J. Sühnel’s comment on the paper: A three-dimensional model to analyze drug–drug interactions, by Prichard MN, Shipman C Jr, in *Antiviral Res* 14:181–206, 1990. *Antiviral Res* 17:95–98
100. Sühnel J (1992) Comment on the paper: A three-dimensional model to analyze drug–drug interactions, by Prichard MN, Shipman C Jr, in *Antiviral Res* 14:181–186, 1990. *Antiviral Res* 17:91–93
101. Sühnel J (1990) Evaluation of synergism and antagonism for the combined action of antiviral agents. *Antiviral Res* 13:23–40
102. Greco WR, Rustum YM (1992) Reply to letters by Berenbaum and Sühnel concerning Greco et al. 1990, in *Cancer Res* 50:5318–5327, 1990. *Cancer Res* 52:4561–4565
103. Sühnel J (1992) Correspondence regarding W R. Greco et al.: an application of a new approach for the quantitation of drug synergism to the combination of cis-diamminedichloroplatinum and 1- $\beta$ -D-arabinofuranosylcytosine. *Cancer Res* 50:5318–5327, 1990. *Cancer Res* 52:4560–4561